



Prevention of SWRO membrane fouling using nano-alumina depth filter

Ibrahim M. El-Azizi^a, Kieran M. Baker^b, Robert G.J. Edyvean^{c,*}

^aDepartment of Power Generating Technologies, Atomic Energy Establishment, Janzour, Tripoli, Libya

^bEarth Surface Science Institute, School of Earth and Environment, University of Leeds, Woodhouse Lane, Leeds LS2 9JT, UK

^cDepartment of Chemical and Biological Engineering, The University of Sheffield, Mappin Street, Sheffield, S1 3JD, UK
Tel. 0044(0)114 222 7506; Fax: 0044(0) 114 2227501; email: r.edyvean@sheffield.ac.uk

Received 23 August 2012; Accepted 1 February 2013

ABSTRACT

This work investigates the effectiveness of seawater pre-treatment for the prevention of membrane fouling during reverse osmosis (RO) using an upstream nano-alumina depth filter. Data from atomic force and scanning electron microscopy, and attenuated total reflectance-Fourier transform infra-red spectroscopy, show that there is a substantial reduction in fouling of RO membranes when a nano-alumina depth filter is used. The filter improved the performance of the RO membranes by removing the majority of substances that cause membrane fouling, including transparent exopolymer particles, micro-organisms and metals. This result demonstrates that nano-alumina filters are an effective and low-cost approach to the pre-treatment of RO membrane systems.

Keywords: Membrane fouling; Nano-alumina depth filter; Pre-treatment

1. Introduction

Fouling is “a condition that resulting in loss of performance of a membrane due to the deposition of suspended and/or dissolved substances on its surface, at its pore openings or within its pores” [1–4]. During the operation of an reverse osmosis (RO) membrane plant, several types of fouling can occur on the membrane surfaces such as inorganic fouling, organic fouling, colloidal fouling and biological fouling “biofouling” [5–7].

Fouling causes a need to increase operating pressure and chemical cleaning which both reduce the membrane life. There is also an increase in energy consumption and thus the cost of RO plant operation [8–10]. In order to maintain the operating performance of a full scale seawater reverse osmosis (SWRO) plant, it is essential to control fouling, which demands an establishment of a comprehensive and practical program of testing and checking of fouling and scaling potential under normal operation conditions [2,11,13,14]. Water sources contain other components such as transparent exopolymer particles (TEP), conditions the surfaces for

*Corresponding author.

Presented at the Conference on Membranes in Drinking and Industrial Water Production. Leeuwarden, The Netherlands, 10–12 September 2012.

Organized by the European Desalination Society and Wetsus Center for Sustainable Water Technology

biofilm development, therefore increasing the biofouling potential in RO membrane systems [15]. TEP are deformable micrometer-sized gel-like particles that form from colloidal polysaccharides and disintegrated micro-organisms [16]. TEPs are rich in surface active acidic polysaccharides, proteins and nucleic acids and are often colonized by bacteria and other micro-organisms [15,16]. TEPs due to their transparent character are not detected by conventional light microscopy alone, and therefore, their role in biofouling of RO membrane systems has not been extensively studied [17]. However, TEP particles were detected during the routine imaging of mucopolysaccharides using Alcian blue staining [16]. A method was therefore developed to measure TEP by staining glass slides that had been suspended in raw seawater for up to 168 h with 0.02% Alcian blue followed by imaging using light microscopy [18]. TEP can be removed from RO feed water depending on the type of pre-treatment system applied upstream to RO membranes. It was reported that in-line coagulation and ultrafiltration (UF) can effectively remove TEP. However, it depends on the coagulation rate and the pore size of UF membranes as TEP particles are flexible and can easily pass through large pore size membranes [19]. In another study [18], it was reported that conventional pre-treatment technology (sand and micron filters) cannot effectively remove TEP.

RO membrane fouling can be reduced by selecting a suitable pre-treatment method. However, due to variations in the water source, conventional pre-treatment requires optimization and development to suit specific requirements, while membrane separation processes require frequent backwashing and chemical cleaning [20–22]. The use of MF/UF membranes upstream of RO membranes increases permeates flux, plant recovery, RO membrane life and decreases chemical cleaning requirements [23–25]. However, they are limited in removing small organic molecules, which are important in the development of biological fouling in RO membrane systems [26].

An alternative pre-treatment process is to use the nano-alumina depth filters marketed under trade name Disruptor™ upstream of the RO membranes. This filter is made from fibres of the electropositive mineral boehmite (AlOOH), which are attached to micro-glass fibres to form a non-woven mat with a surface area of approximately $500\text{ m}^2\text{ g}^{-1}$. This arrangement permits the removal of a variety of submicron contaminants from water through mechanical entrapment and adsorption [27]. Also, the Al^{3+} surface charge extends up to one micron from the end of the fibre, resulting in high electrokinetic potential that attracts and retains the majority of negatively charged, sub-micron particles present in solution. The nano-alumina filter

material can be used as die cut sheets or as stack disc filters, and can be easily pleated for use as cartridge filters. A typical $2.5'' \times 10''$ cartridge has more than $10,000\text{ m}^2$ of active surface area and is capable of removing contaminants and produces filtration efficiency similar to MF and UF membranes but with typical recommended flow rates of 40–140 ($\text{L min}^{-1}\text{ m}^{-2}$).

This study investigates the effectiveness of nano-alumina depth filters as a pre-treatment approach for preventing membrane fouling. The effectiveness of the nano-alumina in protecting RO membranes by removing TEP, micro-organisms upstream of RO membranes was investigated using a laboratory-scale membrane filtration unit.

2. Materials and methods

2.1. Raw seawater

Raw seawater was collected from the coastal North Sea in clean, sterile 20-L containers, transported to the laboratory and stored at 4°C for no more than 24 h. pH (pH meter model HI 8424, Hanna Instruments), conductivity (Model CON 410, OAKTON-Eutech Instruments), total dissolved solids (meter Model CON 410, OAKTON-Eutech Instruments) and temperature were measured prior to the start of the experiments and throughout all experimental runs.

2.2. Filter media

The filter media selected for this study were $5\text{ }\mu\text{m}$ polypropylene cartridge filters and a nano-alumina depth filters. All filters were supplied by Amazon Filtration Ltd., UK.

2.3. RO membrane

The seawater reverse osmosis membrane (RO) used in the fouling experiments was a high pressure, thin film composite (TFC) (TM320–870), provided by Toray Membrane Europe, Switzerland. The RO membranes were provided as flat A4 sheets and were stored at 4°C under dry conditions. Samples were cut to 81 cm^2 and soaked in ultra-pure water for 24 h prior to use. The membranes were characterized atomic force microscopy (AFM) to assess the membrane roughness, attenuated total reflectance Fourier-transform infra-red spectroscopy (ATR-FTIR) for surface functional group analysis, and scanning electron microscopy with energy dispersive spectrometer (SEM-EDS) for bulk chemical analysis and the imaging of fouling material.

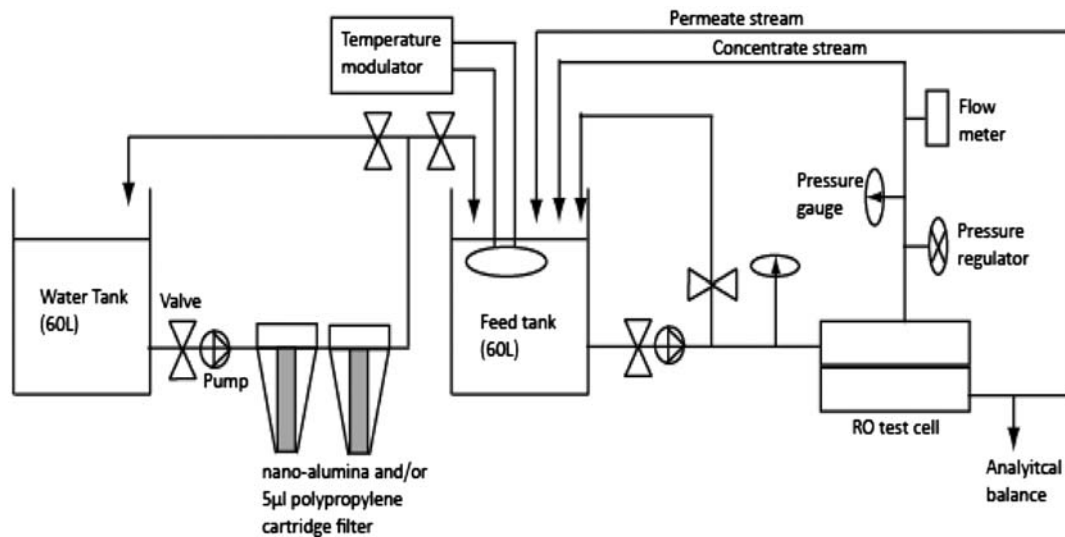


Fig. 1. Schematic diagram of filtration unit and RO test unit (Q_f —feed flow, P_f —feed pressure, Q_c —concentrate flow and Q_p —permeate flow).

2.4. Cross-flow membrane filtration test unit

The laboratory-scale cross-flow membrane filtration unit is shown in Fig. 1. Raw sea water was held in a 60-L polypropylene reservoir and pumped either directly into the cross-filtration RO test cell (Osmonics, Desal, USA) or via the pre-treatment filter cartridges and a feed tank at high pressure (pump model D-03-991-2400A, Hydra-Cell Industrial Pumps, MN, USA). After passing through the RO test cell, the seawater in the both the concentrate and permeate stream was returned to the break tank prior to recycling.

The pressure was controlled using a pressure regulation valve installed on the concentrate side of the RO test cells. The concentrate flow rate (Q_c) was measured using an in-line digital flow meter (Model CZ-32555-04, Cole-Parmer), and the feed (P_f) and concentrate pressures (P_c) were measured by pressure gauges (Model CZ-680022-07, Cole-Parmer, London, UK) connected to the feed and concentrate streams of the RO unit. The flow rate of the permeate stream (Q_p) was measured by weighing sea water samples taken from the stream at timed intervals to ensure consistent operation. Prior to each experimental run, the cross-flow RO filtration unit was cleaned by flushing with 0.1% v/v NaOH (pH 11) for 1 h, 0.1% v/v HCl (pH 3) solution for 1 h, before rinsing with de-ionized water (DI) for 30 min.

2.5. Experimental procedure

RO membranes were placed in the cell unit and rinsed with high-quality RO permeate water (TDS = 5 mg L⁻¹) at a feed pressure of 100 PSI for 30 min to remove any impu-

rities attached to the membrane surface. As the membrane coupons to be tested have a small surface area and would be affected by the compaction under high operating pressure, the permeate flux was measured with high-quality RO permeate water at an operating pressure of 600 PSI and stable temperature ($25 \pm 1^\circ\text{C}$) until a constant flux was achieved. To investigate the effect of composite fouling on permeate flux, raw seawater was pumped directly into the RO test unit containing a conditioned membrane.

To measure permeate flux, each permeate sample was collected over a period of 30 min in a pre-weighed glass beaker and weighed using an analytical balance. Feed and permeate conductivity and pH were also measured during the experiments. The fouled RO membrane samples were carefully removed from the cell, rinsed twice with DI water and dried in a laminar flow cabinet prior to microscopic analysis. At the end of each fouling experiment, the feed tanks were emptied and the cross-flow RO unit was rinsed with high quality RO permeate water. After rinsing, both filtration units were cleaned by flushing with 0.1% v/v NaOH solution (pH 11) for 1 h and 0.1% v/v HCl solution (pH 3) for 1 h. After chemical cleaning, the RO unit was rinsed again with high-quality RO permeate water for 30 min. Each experiment was replicated.

2.6. Permeate flux

Permeate flux (J_w) was calculated as follows [28]:

$$J_w = \frac{Q_p}{A}$$

where Q_p is the permeate flow rate and A is the membrane surface area. Permeate flux is a function of temperature due to viscosity effects and can be corrected to a standard temperature (25°C) using the following equation [29]:

$$J_s = J_A \exp\left(K\left[\frac{1}{298} - \frac{1}{T + 273}\right]\right)$$

where J_s is standard permeate flux, J_A is actual permeate flux, K is temperature coefficient (dependent on the membrane material) and T is temperature (°C). The decline in normalized permeate flux was compared to initial permeate flux, as determined using the following equation [9].

$$\text{Permeate flux decline (\%)} = \left(1 - \frac{J}{J_0}\right) \times 100$$

where J_0 is the initial permeate flux, J is the actual permeate flux taken every 30 min of filtration run.

2.7. Atomic force microscopy

The surface morphology and roughness of clean and fouled RO membranes was examined using a Nanoscope III atomic force microscope (Digital instruments, USA). Imaging was carried out in tapping mode. Standard Nanoprobe Silicon (Si) cantilevers (model OMCL-AC160TS-E) were used. The probe has a nominal cantilever length of 160 μm, a nominal tip radius of 7 nm, a spring constant of 42 N/m and resonant frequency of 300 kHz. The clean and fouled RO membrane coupons were dried in a vacuum prior to the AFM scan.

2.8. SEM-EDS

A SEM (FEI Quanta 200 SEM, FEI, USA) fitted with EDS was used for surface morphology and elemental analysis of fouling material on the RO membrane surfaces. 1 cm² membrane coupons were cut from the clean and fouled nano-alumina depth filter and RO membranes, dried in a flow cabinet and mounted on the test disc and coated with gold prior to imaging and elemental analysis. Wide-scan spectra were collected at a fixed accelerating voltage of 500 kV to assess the elemental composition of the fouling material. SEM images were taken at 4,000× and 25,000× magnifications.

2.9. ATR-FTIR

Clean and fouled nano-alumina and RO membrane samples were analysed for surface functional groups

using ATR-FTIR (PerkinElmer FTIR spectroscope—USA). To reduce the interference of water, samples were air-dried prior to ATR-FTIR measurements. The filters and membrane samples were pressed against each side of a germanium (Ge) reflection element (6 mm, 45°). All spectra were recorded with 100 scans and a wave number resolution of 4 cm⁻¹.

2.10. Quantification of transparent exopolymer particles (TEP) and attached microbes

TEP particles were measured in raw and pre-filtered seawater according to the method described by Bar-Zeev et al. [18]. Three sterile glass microscope slides were suspended in beakers containing 500 mL of raw and pre-filtered SW and incubated at 25°C in a rotary shaker at 100 rpm. Slides were removed after 48, 72 and 168 h and transferred into sterile agar plates, stained with 0.02% Alcian blue for 7 min, and rinsed twice with sterile distilled water to remove excess dye. The slides were covered until imaging using a light microscope (Zeiss Axioplan 2, Carl Zeiss Ltd. UK). 20 fields of view were imaged at 20× magnification.

Micro-organisms attached to the slides were also imaged and enumerated. Microbial cells were stained with 10 μL of 4',6-diamidino-2-phenylindole (DAPI, concentration 3 μg mL⁻¹) for 7 min in the dark. A drop of mounting oil (Olympus, Fisher Scientific, UK) and a cover slip was placed onto the glass slide, before imaging using epifluorescence microscopy. Images of 20 fields of view were collected at 100× magnification and the number of DAPI-stained microbes was normalized to cells cm⁻².

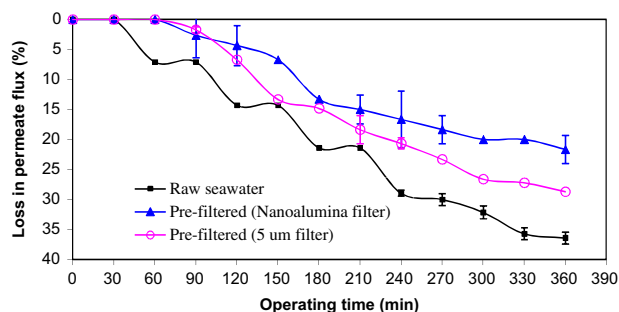


Fig. 2. Comparative permeate flux decline of untreated seawater and seawater pre-filtered through the 5 μm filter, the nano-alumina pre-filter.

3. Results and discussion

3.1. The effect of composite fouling on permeate flux

Fig. 2 shows percentage permeate flux decline over time throughout the filtration experiments. Pumping unfiltered (raw) seawater through the RO membrane results in a rapid decline in permeate flux after 30 min. The permeate flux decreased further over time due to an increase in fouling. By the end of the experiment, the permeate flux declined by 43.8%. Foulants in the raw seawater accumulated on the membrane surface. This increases hydraulic resistance to permeate flow and results in the decline in permeate flux.

Permeate flux of seawater was similar when pre-filtered through either the 5 μm filter or the nano-alumina filter, remaining stable in the first 90 min (zero loss in permeate flux). After this period, deviations occurred, and by the end of the experiment, permeate flux of the seawater pre-filtered through the 5 μm cartridge filter decreased by 27% compared with 21% loss for seawater pre-filtered through the nano-alumina filter. Accordingly, data suggest that pre-treatment of seawater with the nano-alumina depth filter alone results in a lower decline in permeate flux in comparison to the 5 μm pre-filter.

3.2. Atomic force microscopy

The types of foulants that deposit on the membrane surface during reverse osmosis and the surface morphologies of clean and fouled RO membranes were investigated using atomic force microscopy (AFM). Figs. 3 and 4(a) show the effects of raw seawater fouling on the surface of a membrane. The surface becomes covered by scaling, micro-organisms and clusters of densely packed particles, resulting in a

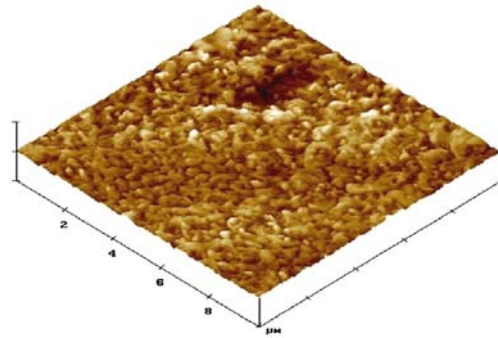


Fig. 3. 3D AFM topography of a clean RO membrane.

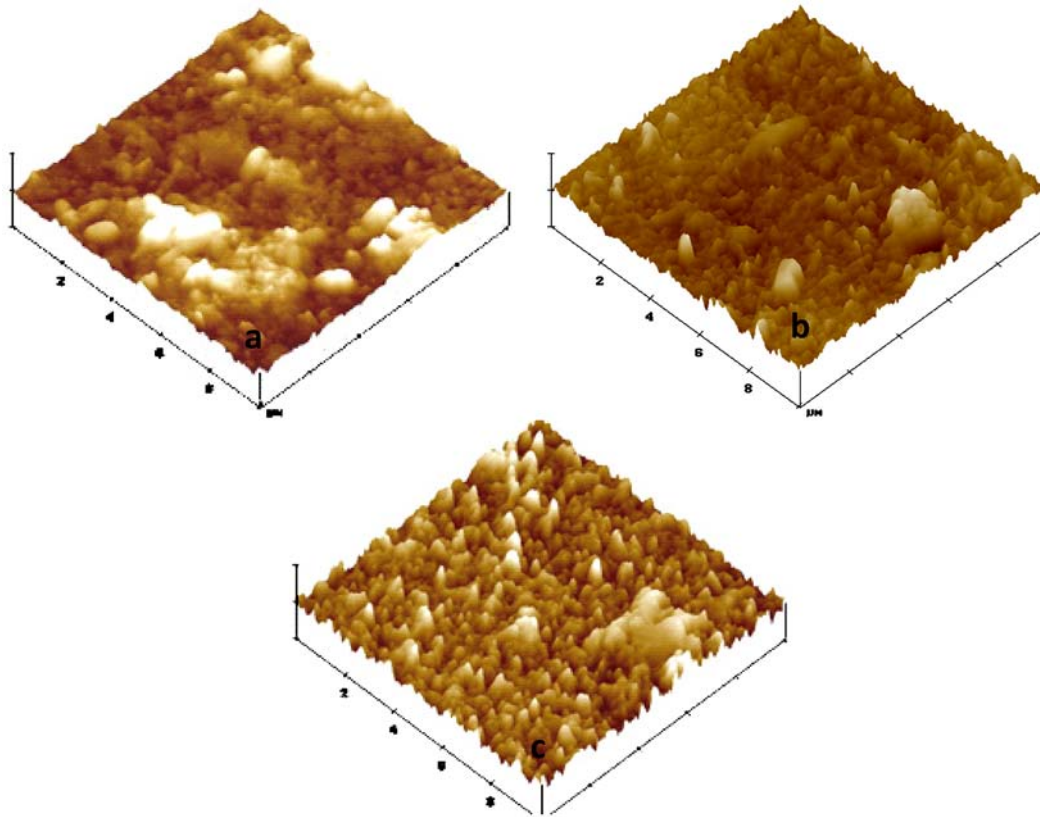


Fig. 4. 3D AFM topography of fouled RO membrane by raw seawater (a), sea water pre-filtered through the 5 μm cartridge filter alone (b), and pre-filtered through the nano-alumina depth filter alone (c).

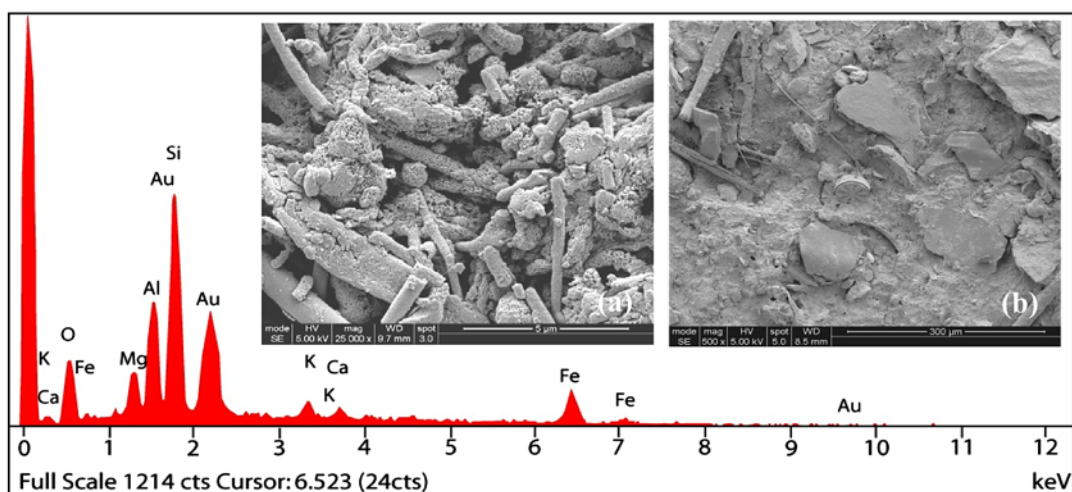


Fig. 5. SEM images of clean (a) and fouled nano-alumina filter (b) and its (c) EDS spectrum of fouled filter.

change the membrane surface morphology (Fig. 4(a)). This creates a rougher membrane surface (in comparison to a clean membrane) that further enhances foulant attachment [30,31].

The AFM image of the RO membrane receiving seawater that was pre-filtered through the 5 μm cartridge filter (Fig. 4(b)) shows micro-organisms and scaling on the membrane surface. This indicates that a 5 μm filter has limitations in protecting the RO membrane from biofouling. However, seawater pre-filtered through the nano-alumina filter only (Fig. 4(c)) showed only slight scaling.

AFM investigations demonstrate the high efficiency of the nano-alumina filter to pre-treat the raw seawater. Results show that the majority of foulants were removed from the feed water and only slight

scaling was detected. Scaling problems due to concentration polarization can be prevented by adjusting seawater pH or the addition of antiscalants to the RO feed water. AFM results also show that combining both pre-treatment options (5 μm filter and nano-alumina filter) greatly reduces the fouling of the RO membrane, suggesting that combining the two pre-filtration technologies will extend RO membrane life and performance.

3.3. SEM-EDS

SEM imaging and EDS was performed to investigate the surface morphology and to assess surface elemental composition of both clean and fouled nano-alumina filters (Fig. 5). Deposits of a thick

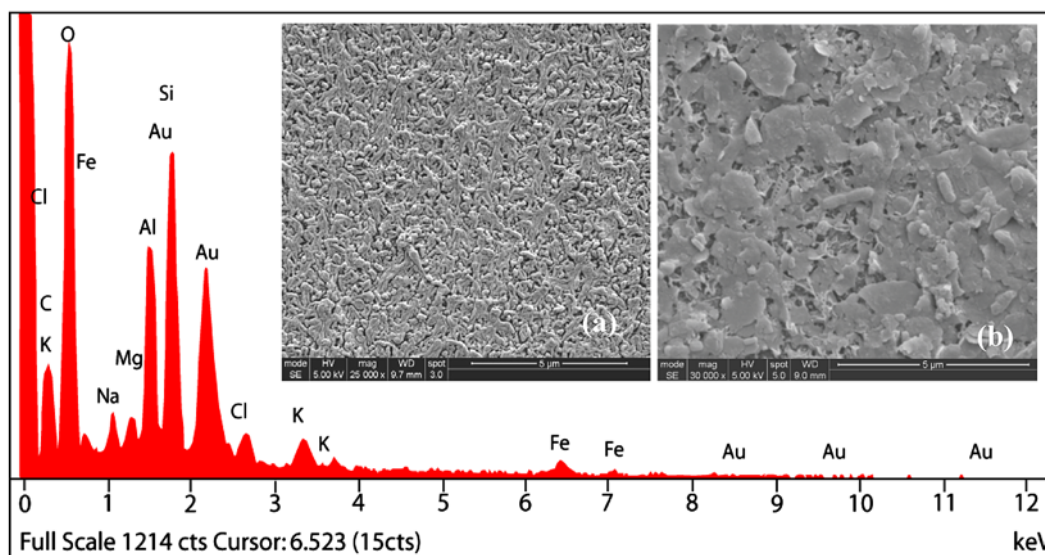


Fig. 6. SEM images of a clean (a) RO membrane and (b) a RO membrane after fouling by raw seawater and its EDS spectrum.

fouling layer on the surface containing scaling, colloids and micro-organisms (Fig. 5(b)) form with exposure to raw seawater. The EDS spectrum shows that the major elements of inorganic foulants are iron, aluminium, silica and calcium. This suggests that the alumina filter has the capability to remove particles, colloids, micro-organisms and dissolved (or trapped) metals.

SEM micrographs of a clean and a raw seawater fouled RO membrane (Fig. 6) show that the membrane will become covered by a similar layer of scaling, colloids and micro-organisms on exposure to raw seawater (Fig. 6(b)). The EDS spectrum of the fouled RO membrane shows that the elemental composition of the fouling is similar to that removed by the nano-alumina filter.

Adsorption and deposition of colloidal particles and organic substances are thought to cause the first fouling layer [29,30]. This layer then accelerates the formation of other types of fouling. Formation of more than one type of fouling increases the degree of concentration polarization on the membrane surface, leading to a rapid permeate flux decline and an increase in differential pressure and salt passage. SEM micrographs and EDS spectra of the RO membranes fouled by seawater pre-filtered through the 5 μm filter show that the amount of fouling is higher than on the RO membrane fouled by seawater pre-filtered through a nano-alumina filter (Fig. 7(a) and (b)).

The SEM micrographs of both membranes look identical to the clean membrane and only slight scaling is visible. The EDS spectrum shows the presence of only Na and Cl, with a “cleaner” spectrum for the

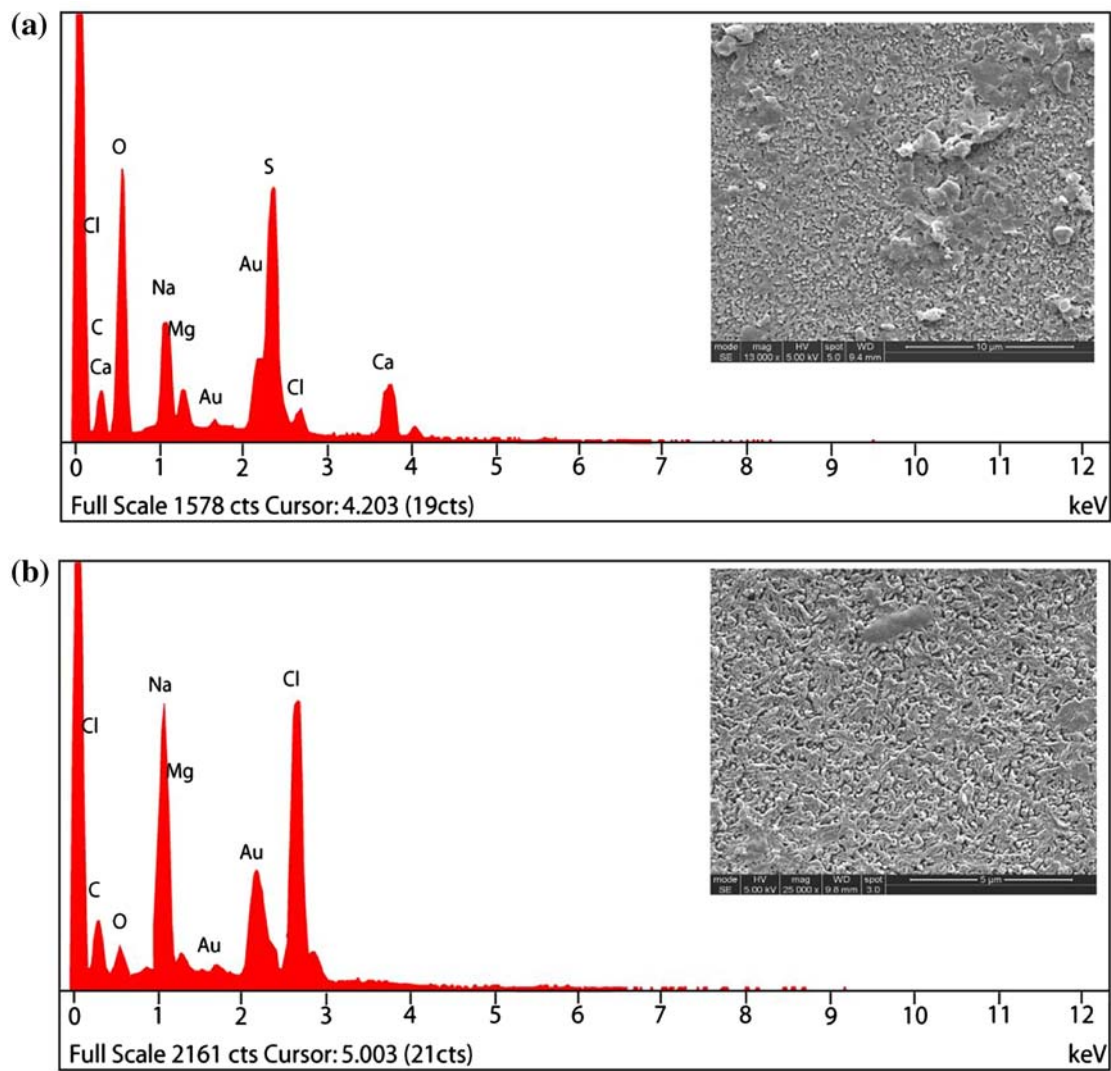


Fig. 7. SEM micrographs and EDS spectra of RO membrane fouled by seawater pre-filtered through the 5 μm filter alone (a) and through the nano-alumina filter alone (b).

membrane after both 5 μm and nano-alumina filters than by either alone. These data show that a nano-alumina filter can remove the majority of substances that may foul RO membranes. Therefore, this media can be used as an effective pre-treatment for RO membrane systems.

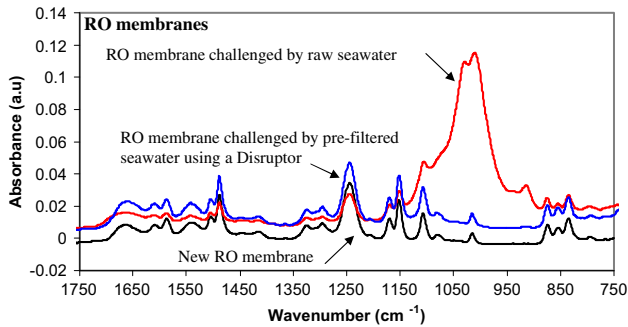


Fig. 8. ATR-FTIR spectra of clean and fouled nano-alumina filter (top) and RO membranes (bottom).

3.4. ATR-FTIR

ATR-FTIR was used to investigate the surface chemical functional groups of both clean and fouled RO membranes. ATR-FTIR spectra (Fig. 8) reveal that the high absorption bands on the RO membrane fouled by raw seawater are reduced in comparison with the clean RO membrane. This is a result of the fouling layer seen using SEM. Some peaks can be detected through the fouling layer, suggesting that the fouling layer is less than 5 μm thick. The fouled nano-alumina filter and RO membrane show similar strong peaks in the region between 1,100 and 900 cm^{-1} , suggesting that the foulants are likely to be protein, polysaccharides and silicate colloids [30–32], indicating both biofouling and colloidal fouling. However, the spectra of a clean RO membrane and an RO membrane fouled by seawater pre-filtered through a nano-alumina filter show similar spectra with no such peaks. This again indicates that the nano-alumina filter removed the majority of foulants from the RO feed water and thus protects the RO membrane from fouling.

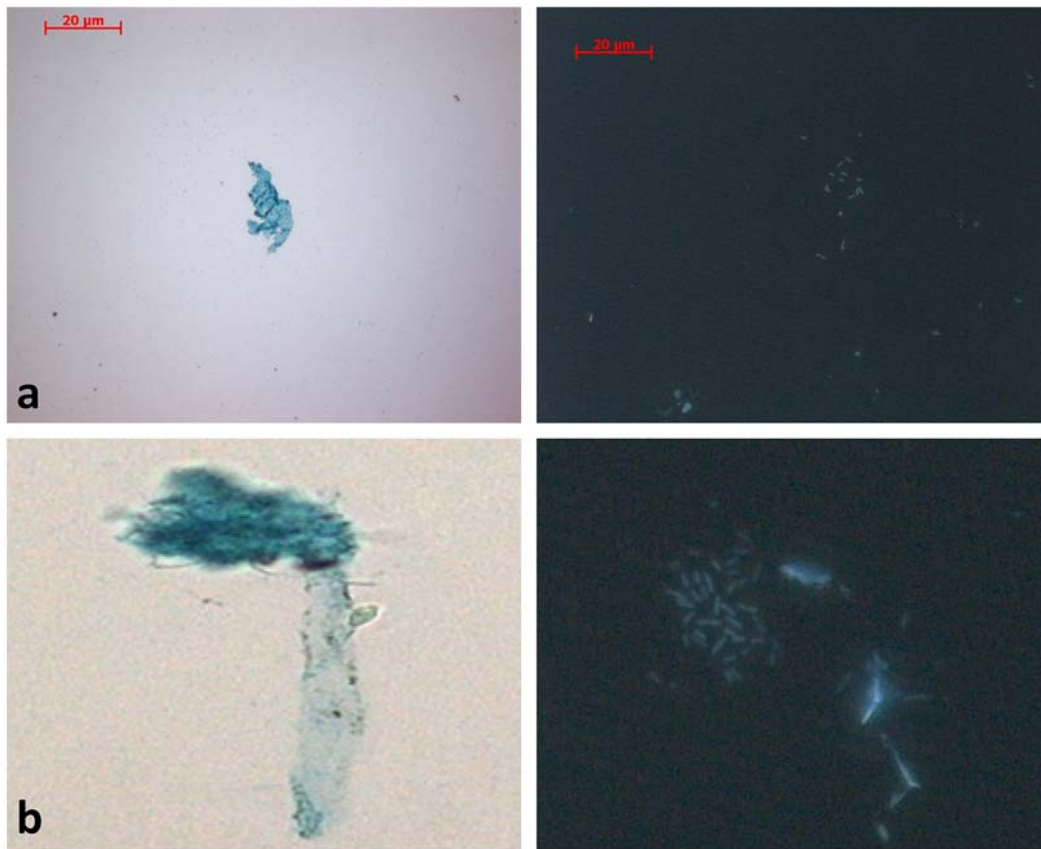


Fig. 9. Images of TEP (left) and fluorescently labelled microbial cells attached to glass slides suspended in untreated seawater after 24 h (a) and 168 h (b) of incubation. Scale bar applicable to all images.

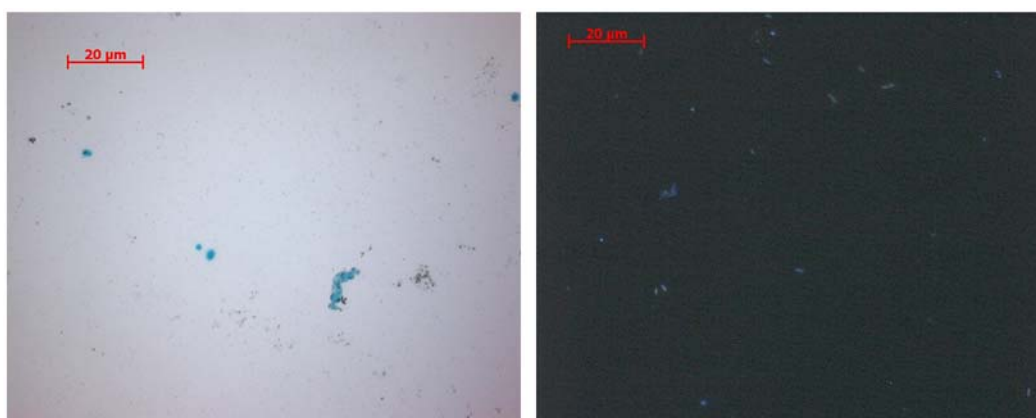


Fig. 10. Images of TEP (left) and fluorescently labelled microbial cells after 168 h of incubation in sea seawater pre-filtered through nano-alumina filter.

3.5. TEP particles

The size and number of TEP particles in raw and pre-filtered seawater were investigated. After 24-h incubation, small particles of TEP and a few bacteria were found on the glass slides suspended in the raw seawater (Fig. 9(a)). After 168 h of incubation, the TEP were larger in size and a high number of bacteria were observed (Fig. 9(b)). The results indicate that the presence of TEP in the water increases biofouling potential and biofilm development. Similar results were reported by Bar-Zeev et al. [18] where the size of stained TEP and number of bacteria increased with incubation.

Seawater pre-filtered through a nano-alumina filter contained very small TEP and no microbial cells in the first 24 h of incubation. After 168 h, TEP particles had not increased in size, and cells remained almost undetectable (Fig. 10(a) and (b)).

4. Conclusions

Laboratory-scale fouling experiments were carried out to investigate the performance of 5 μm cartridge and nano-alumina pre-filters in reducing RO membrane fouling. Results show a considerable improvement in the performance of RO membranes when using the nano-alumina pre-filter or a combination of 5 μm and nano-alumina pre-filters to treat raw seawater when compared to either no pre-filtration or pre-filtration using a 5 μm polypropylene filter alone. Stable permeate flux was achieved, highlighting that the pre-treatment of seawater using a nano-alumina filter can extend the optimum performance lifetime of RO membranes. This reduces the requirement for frequent chemical cleaning, resulting in reduced

operating costs. AFM, SEM and ATR-FTIR results demonstrate that a nano-alumina filter is highly efficient at removing fouling material. Moreover, it was found that the nano-alumina filter can remove around 80% of TEP, which are responsible for biofouling and biofilm development. It can be concluded that the pre-treatment of raw seawater with a nano-alumina filter can substantially reduce the severity of fouling and biofilm formation in SWRO membrane systems.

Acknowledgement

The authors would like to thank Ahlstrom Filtration LLC, USA and Amazon Filtration Ltd. UK for supporting this study.

References

- [1] S. Lee, L. Cho, M. Elimelech, Influence of colloidal fouling and feed water recovery on salt rejection of RO and NF membranes, *Desalination* 160 (2004) 1–12.
- [2] S. Lee, W.S. Ang, M. Elimelech, Fouling of reverse osmosis membrane by hydrophilic organic matter: implications of water reuse, *Desalination* 187 (2006) 313–321.
- [3] M. Kumar, S.S. Adham, W.R. Pearce, Investigation of seawater reverse osmosis fouling and its relation to pre-treatment type, *Environ. Sci. Technol.* 40 (2006) 2037–2044.
- [4] T. Darton, U. Annunziata, F.V. Vigo Pisano, S. Gallego, Membrane Autopsy Helps to Provide Solutions to operational Problems, *Desalination* 167 (2004) 239–245, M. Herzberg and M. Elimelech, Biofouling of reverse osmosis membranes: Role of biofilm-enhanced osmotic pressure, *J. Membr. Sci.*, 295 (2007) 11–20.
- [5] M.A. Saad, Early discovery of RO membrane fouling and real-time monitoring of plant performance for optimising cost of water, *Desalination* 183 (2004) 188–191.
- [6] H.K. Shon, S.H. Kim, S. Vigneswari, R. Ben Aim, D. Lee, J. Cho, Physicochemical pre-treatment of seawater: Fouling reduction and membrane characterisation, *Desalination* 238 (2009) 10–21.

- [7] J.S. Vrouwenvelder, D. Van der Kooij, Diagnosis of fouling problems of NF and RO membrane installation by a quick scan, *Desalination* 153 (2002) 121–124.
- [8] J.S. Vrouwenvelder, J.W.N.M. Kappelhof, S.G.J. Heijman, J.C. Schippers, D. van der Kooij, Tools for fouling diagnosis of NF and RO membranes and assessment of the fouling potential of feed water, *Desalination* 157 (2003) 361–365.
- [9] P. Xu, J.E. Drewes, T. Kim, C. Bellona, G. Amy, Effect of membrane fouling on transport of organic contaminants in NF/RO membrane applications, *J. Membrane Sci.* 179 (2006) 165–175.
- [10] S.S. Mitra, A.R. Thomas, G. Tian Gang, Evaluation and characterization of seawater RO membrane fouling, *Desalination* 249 (2009) 94–107.
- [11] V. Bonnelye, M.A. Sanx, J. Durand, L. Plasse, F. Gueguen, P. Mazounie, Reverse osmosis on open intake seawater: pretreatment strategy, *Desalination* 167 (2004) 191–200.
- [12] C. Park, Y.H. Lee, S. Lee, S. Hong, Effect of cake layer structure on colloidal fouling in reverse osmosis membranes, *Desalination* 220 (2008) 335–344.
- [13] T. Berman, M. Holenberge, Don't fall foul of biofilm through high TEP levels, *Filtrat. Separat.* 42 (2005) 30–32.
- [14] U. Passow, R.F. Shipe, A. Murray, D.K. Pak, M.A. Brzezinski, A.L. Alldredge, The origin of transparent exopolymer particles (TEP) and their role in the sedimentation of particulate matter, *Cont. Shelf Res.* 21 (2001) 327–346.
- [15] M.D. Kennedy, F.P.M. Tobar, G. Amy, J.C. Schippers, Transparent exopolymer particle (TEP) fouling of ultrafiltration membrane systems, *Desalin. Water Treat.* 6 (2009) 169–176.
- [16] E. Bar-Zeev, I.B. Frank, B. Liberman, E. Raha, U. Passo, T. Berman, Transparent exopolymer particles: potential agents for organic fouling and biofilm formation in desalination and water treatment plants, *Desalin. Water Treat.* 3 (2009) 136–142.
- [17] L.O. Villacorte, R. Schurer, M. Kennedy, G.L. Amy, J.C. Schippers, The fate of transparent exopolymer particles (TEP) in seawater UF-RO system: A pilot plant study in Zeeland, The Netherlands, in: Conference and Exhibition in Desalination for the Environment, Clean Water and Energy Conference, 17–20 May 2009, Baden-Baden, Germany.
- [18] R.J. Xie, E.K. Tan, S.K. Lim, E. Haw, C.P. Chiew, A. Sivaraman, A.N. Puah, Y.H. Lau, C.P. Teo, Pre-treatment optimization of RO membrane desalination under tropical conditions, *Desalin. Water Treat.* 3 (2009) 136–142.
- [19] M. Kumar, S.S. Adham, W.R. Pearce, Investigation of seawater reverse osmosis fouling and its relation to pretreatment type, *Environ. Sci. Technol.* 40 (2006) 2037–2044.
- [20] H.K. Shon, S.H. Kim, S. Vigneswaran, R. Ben Aim, S. Lee, J. Cho, Physicochemical pretreatment of seawater: Fouling reduction and membrane characterization, *Desalination* 238 (2009) 10–21.
- [21] A. Teuler, K. Glucina, J.M. Iain, Assessment of UF pre-treatment prior RO membranes for seawater desalination, *Desalination* 125 (1999) 89–96.
- [22] M. Wilf, M.K. Schierach, Improved performance and cost reduction of RO seawater systems using UF pretreatment, *Desalination* 135 (2001) 61–68.
- [23] V. Bonnelye, L. Guey, J. Del Castillo, UF/MF as RO pre-treatment: the real benefit, *Desalination* 222 (2008) 59–65.
- [24] K.A. Bu-Rashid, W. Czolkoss, Pilot tests of multibore UF membrane at Addur SWRO desalination plant, Bahrain, *Desalination* 203 (2007) 229–242.
- [25] G.M. Priel, M. Wilf, Field evaluation of capillary UF technology as a pretreatment for large seawater RO systems, *Desalination* 147 (2002) 55–62.
- [26] F. Tepper, I. El-Azizi, Nano-alumina pre-filters for reduction of fouling on RO, in: Annual conference and exposition, Improving American's Waters through Membrane Filtration and Desalting, 13–16 July 2009, Austin—Texas, USA.
- [27] B.A.Q. Darwish, M. Abdel-Jawad, G.S. Alyon, The standardization of performance data for RO desalination plants, *Desalination* 74 (1989) 125.
- [28] M. Elimelech, X. Zhu, E.C. Amy, S. Hong, Role of membrane surface morphology in colloidal fouling of cellulose acetate and composite aromatic polyamide reverse osmosis membranes, *J. Membr. Sci.* 127 (1997) 101–109.
- [29] V. Freger, J. Gilron, S. Belfer, TFC polyamide membranes modified by grafting of hydrophilic polymers: An FT-IR/AFM/TEM study, *J. Membr. Sci.* 209 (2002) 283–292.
- [30] Rene Schneider Peter, Liutas Martinaitis, Paula Binder, Jose Ramos, Robert Analysis of foulant layer in all elements of an RO train, *J. Membr. Sci.* 261 (2005) 152–162.
- [31] J. Cho, G. Amy, J. Pellegrino, Y. Yoon, Characterisation of clean and natural organic matter (NOM) fouled NF and UF membranes, and foulants characterization, *Desalination* 118 (1998) 101–108.